

# **N<sub>2</sub>O Production Characteristics of Ammonia/Hydrogen/Air Premixed Laminar Flames Stabilized in Stagnation Flows at Lean Conditions**

**Akihiro Hayakawa<sup>1</sup>, Masao Hayashi<sup>1,2</sup>, Gabriel J. Gotama<sup>1</sup>, Marina Kovaleva<sup>3</sup>, Ekenechukwu C. Okafor<sup>4</sup>,  
Sophie Colson<sup>1</sup>, Taku Kudo<sup>1</sup>, Syed Mashruk<sup>3</sup>, Agustin Valera-Medina<sup>3</sup>, Hideaki Kobayashi<sup>1</sup>**

<sup>1</sup>Institute of Fluid Science, Tohoku University

2-1-1 Katahira, Aoba-ku, Sendai, Miyagi 980-8577, Japan

<sup>2</sup>Department of Aerospace Engineering, Tohoku University

6-6-1, Aoba, Aramaki, Aoba-ku, Sendai, Miyagi 980-8579, Japan

<sup>3</sup> College of Physical Sciences and Engineering, Cardiff University

Queen's Building, Cardiff CF24 3AA, United Kingdom

<sup>4</sup> Fukushima Renewable Energy Institute, National Institute of Advanced Industrial Science and Technology

2-2-9 Machiikedai, Koriyama, Fukushima 963-0298, Japan

## **Abstract**

Product gas characteristics of ammonia/hydrogen/air laminar premixed flames stabilized in stagnation flows were experimentally and numerically studied. The maximum value of NO mole fraction increased compared with pure ammonia/air flames, and a trade-off relationship between NO and unburnt NH<sub>3</sub> was observed. In addition, the N<sub>2</sub>O production for very lean conditions was observed. To clarify the N<sub>2</sub>O production mechanism in detail, numerical simulations were employed using CHEMKIN software with the reaction kinetics developed by Gotama et al. Sensitivity analysis suggested that the reactions of (R58) NH+NO = N<sub>2</sub>O+H, (R105) N<sub>2</sub>O+H = N<sub>2</sub>+OH, and (R106) N<sub>2</sub>O(+M) = N<sub>2</sub>+O(+M) play an important role in N<sub>2</sub>O mole fraction. Product gas characteristics of N<sub>2</sub>O were numerically investigated for various stagnation plane temperatures and equivalence ratios. The reaction rate of R106 decreases for low stagnation plane temperature and at small equivalence ratios. It was found that the decrease in the reaction rate of R106 hinders the reduction rate of N<sub>2</sub>O to N<sub>2</sub>, and thus large amount of N<sub>2</sub>O were detected. Also, the N<sub>2</sub>O amount decreased when the stagnation plane temperatures were sufficiently high. This also suggested that the N<sub>2</sub>O production may be restricted by a decrease in the heat loss in an ammonia-fueled combustor.

## **1 Introduction**

Reduction in the emission of greenhouse gases, in particular carbon dioxide, is an urgent issue to prevent climate change which is a critical issue as well as one of the development targets of the sustainable development goals (SDGs). To achieve carbon neutrality by 2050, the Japanese government

proposed the Green Growth Strategy. In this strategy, the application of ammonia as fuel is proposed [1]. To reduce CO<sub>2</sub> from combustors, many fundamental studies have been carried out [2], anticipating the application of ammonia as a fuel.

There are mainly two challenges to be solved, towards the application of ammonia in a combustor, especially for a gas turbine. One of these challenges is flame stability caused by the lower burning velocity of ammonia. The maximum laminar burning velocity of ammonia/air flame is almost 1/5 of that of methane/air flame [3]. To increase the laminar burning velocity without adding CO<sub>2</sub> emission, the addition of hydrogen to create ammonia/hydrogen binary fuel is promising strategy. Ichikawa et al. [4] and Gotama et al. (submitted to Combust. Flame, under review), and many other researchers proposed an increase in laminar burning velocity with an increase in the hydrogen fraction in binary fuel of ammonia/hydrogen. However, hydrogen addition changes emission characteristics, which is another challenge for ammonia application as emissions must be adhere to the emission regulation. Fuel NO<sub>x</sub> and unburnt ammonia may be formed when the combustion conditions are not appropriate [5]. Recently, Okafor et al. [6] clarified that the heat loss from the combustor increases N<sub>2</sub>O emission. Since N<sub>2</sub>O has a large global warming potential around of 300 [7], N<sub>2</sub>O emission from combustor must be reduced. To do so, it is important to understand the the fundamental production mechanism of N<sub>2</sub>O.

The objective of this study is to clarify the product gas characteristics of ammonia/hydrogen/air premixed laminar flames stabilized in a stagnation flow. The product gas characteristics are experimentally analyzed. Then, emission characteristics are discussed in detail by conducting a numerical simulation study using a detailed reaction kinetics.

## **2 Experimental Setup**

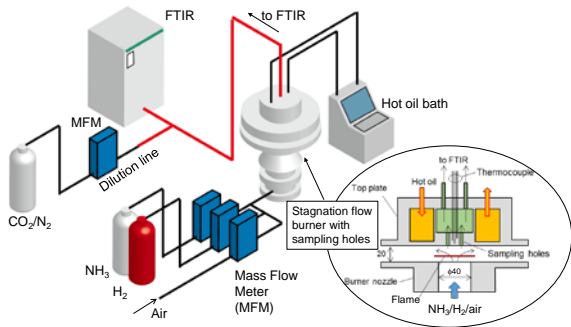


Figure 1: Experimental setup.

Figure 1 shows the schematic of the experimental setup. A similar setup was employed for the product gas analysis of ammonia/air premixed flames [5]. Ammonia and hydrogen were used as fuel, and air was used as an oxidizer. The mixtures were introduced to a nozzle burner with 40 mm outlet diameter, and a top plate being mounted 20 mm above the nozzle burner that generate a stagnation flow. There were sampling holes on the top plate, and the product gas was sucked through the holes. The product gas was introduced to an FTIR (Fourier transform infrared) gas analyzer (BOB-2000FT, Best Instruments). To avoid condensation of water inside the sampling line, the temperature of the sampling line was maintained above 100 °C. The temperature of the top plate was maintained by using hot oil supplied by the hot oil bath. Three thermocouples inserted in the top plate enabled the estimation of the surface temperature of the top plate,  $T_w$ . The value of  $T_w$  was varied depending on the equivalence ratio between and 490.7 K and 583.3 K.

The hydrogen fraction in the binary fuel,  $\zeta_{H_2}$ , was determined as  $\zeta_{H_2} = [H_2]/([H_2]+[NH_3])$ , here  $[X]$  represents the mole fraction of the species  $X$  [4]. The hydrogen fraction was set to 0.3 as suggested by [8] in this study. All experiments were conducted at atmospheric pressure condition. The mixture inlet temperature was  $295 \pm 2$  K. The mixture inlet velocity,  $U_{in}$ , was varied because the laminar burning velocity changes depending on the equivalence ratio between 23.6 cm/s and 44.5 cm/s.

A dilution sampling method was employed when the concentration of the product gas exceeded the measurement range of the FTIR gas analyzer. As shown in Fig. 1, the product gas was diluted by the dilution gas upstream of the FTIR gas analyzer.  $CO_2/N_2$  mixture with  $CO_2$  mole fraction of 15.9 % was employed as the dilution gas. Since  $CO_2$  is not present in the product gas (if the  $CO_2$  from air is neglected),  $CO_2$  was available as a tracer species. The dilution ratio and actual concentration of the product gas were evaluated using the measured concentration of  $CO_2$  in the mixture introduced to FTIR gas analyzer. The detailed descriptions of the dilution sampling method are available elsewhere [9].

Numerical simulations were conducted using ANSYS CHEMKIN software [10]. The premixed laminar burner stabilized stagnation flame model was used to simulate this experiment. As for the reaction model, a detailed reaction model developed by Gotama et al. (referred as Gotama Mech in this paper, submitted to Combust. Flame, under review) was employed. This reaction kinetics were validated in terms of the laminar burning velocity of ammonia/hydrogen/air flames for various equivalence ratios up to 0.5 MPa. The mixture inlet velocity and the stagnation plane temperature are required for the numerical simulation with the strain stabilized model. The estimated values of the surface temperature of the top plate and mixture inlet velocity changed depending on the equivalence

ratio with experimental fluctuation. To determine the boundary condition for the numerical simulation, fitting curves by 5th and 6th polynomials were employed for  $T_w$  and  $U_{in}$ , respectively. Calculated values using the polynomials were used for the boundary condition of the stagnation plane temperature and mixture inlet velocity.

## 3 Results and Discussions

### 3.1 Experimental and Numerical Results

Figure 2 shows the measured product gas characteristics of ammonia/hydrogen/air flames in terms of equivalence ratio,  $\phi$ . The maximum NO mole fraction,  $X_{NO}$ , of around 8700 ppm was observed at  $\phi \sim 0.85$ . This maximum value was larger than that of pure ammonia/air premixed flames whose value was around 3500 ppm within the conditions examined by Hayakawa et al. [5]. The NO mole fraction changes non-monotonically with equivalence ratio, and almost no emission was observed around  $\phi > 1.20$ . However, the emission of unburnt  $NH_3$  were also increased around this equivalence ratio. At rich condition, trade-off relationship between NO and unburnt  $NH_3$  emissions were observed. The optimal equivalence ratio at which NO and unburnt ammonia emissions reach minimum simultaneously can be determined. The optimal equivalence ratio was found to be at around  $\phi \sim 1.20$ , and was larger than that for the case of pure ammonia/air flames [6]. As shown in Fig. 2e, hydrogen was detected in the product gas at rich condition, and hydrogen mole fraction increases with an increase in the equivalence ratio, that reached high as  $\sim 8\%$  within the examined conditions in this study. The trade-off characteristics between NO and unburnt  $NH_3$  at rich condition can be applied the rich-lean two stage combustor in ammonia-

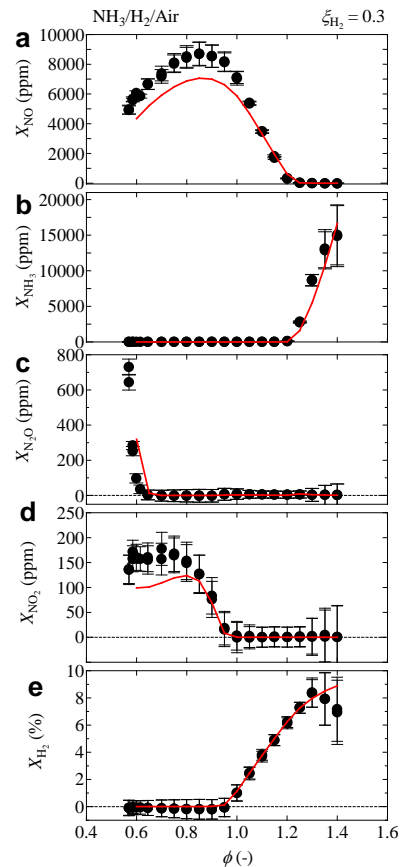


Figure 2: Experimental and numerical results of product gas characteristics of ammonia/hydrogen/air laminar premixed flames of (a) NO, (b)  $NH_3$ , (c)  $N_2O$ , (d)  $NO_2$ , and (e)  $H_2$ . Here,  $X_i$  represents the mole fraction of species  $i$ .

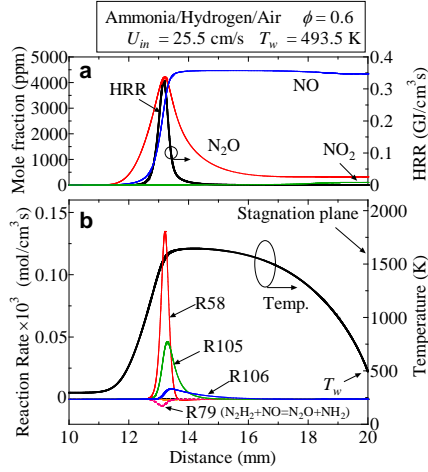


Figure 3: Flame structure of ammonia/air/hydrogen flame at  $\phi = 0.6$ . The mixture inlet velocity and the stagnation plane temperature were the same with the experimental condition.

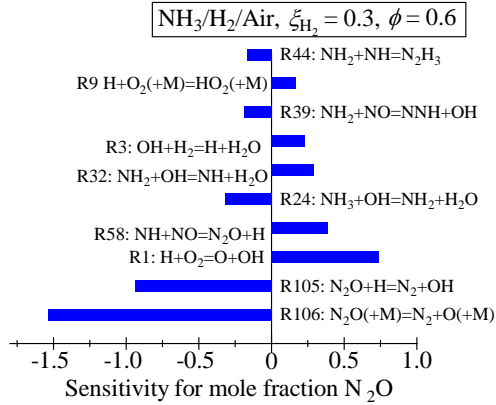


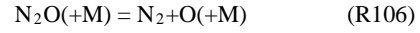
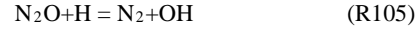
Figure 4: Sensitivities for mole fraction of  $N_2O$  for  $\phi = 0.6$  at the stagnation plane. The mixture inlet velocity and the stagnation plane temperature were the same with the experimental condition.

fueled gas turbine combustor to allow simultaneous reduction in  $NO_x$ , unburnt ammonia, and hydrogen.

As shown in Fig. 2d,  $NO_2$  was detected for lean condition, and the value increases around 170 ppm. It was also noted that a significant increase in  $N_2O$  was detected for lower equivalence ratio conditions of  $\phi \sim 0.6$  as shown in Fig. 2c. Because of the large global warming potential of  $N_2O$ , the equivalence ratio range with large  $N_2O$  production should not be employed for a combustor.

The numerical results calculated using the Gotama Mech were also shown in Fig. 2 with red curves. Although the calculated values predict slightly lower values for  $NO$  and  $NO_2$  than the experimental values, it was considered that product gas characteristics were well predicted by the Gotama Mech.

Figure 3 shows the flame structure at  $\phi = 0.6$ . Gotama Mech has 6 elementary reactions that express  $N_2O$  production or reduction. Figure 3b represents the reaction rate of the reactions express  $N_2O$  production or reduction in Gotama Mech. In addition, Fig. 4 shows the sensitivity of  $N_2O$  at the stagnation plane, i.e., the end point of computational domain. According to these results, it was considered that these three elementary reactions play an important role in  $N_2O$  production:



where R represents the reaction number in the Gotama Mech. R58 is the  $N_2O$  production path from  $NO$ , and  $N_2O$  was reduced to  $N_2$  through R105 and R106. In this paper, these reactions were discussed to understand the  $N_2O$  production and reduction mechanisms.

### 3.2 Effects of Top Plate Temperature on Product Gas Characteristics

As indicated by Okafor et al. [6],  $N_2O$  emission occurs when the low temperature region exists in the combustion field due to such as heat loss. Thus, the numerical simulations were conducted for various stagnation plane temperature,  $T_w$ , with the fixed mixture inlet velocity at the equivalence ratio of  $\phi = 0.6$ . Figure 5 shows calculated  $N_2O$  mole fraction at the stagnation point for various stagnation plane temperature at  $\phi = 0.6$ . The mole fraction of  $N_2O$  decreased with an increase in the stagnation plane temperature, and  $N_2O$  reached almost zero for  $T_w > 1700$  K. This indicates that  $N_2O$  emission may be restricted when heat loss can be reduced in an ammonia-fueled combustor. However, in the case of an actual combustor, wall material temperature limitations must also be considered.

Figure 6 shows the variation of the integral value of the reaction R,  $I_R$ . Here, the value of  $I_R$  was calculated using Eq. (1),

$$I_R = \int_0^L \dot{\omega}_R dx \quad (1)$$

where  $L$  represents the distance from the burner outlet and the top plate,  $\dot{\omega}_R$  is the reaction rate of reaction R, and  $x$  is the distance. The value of  $I_{R58}$  represents  $N_2O$  production through R58, and  $I_{R105}$  and  $I_{R106}$  represent  $N_2O$  reductions through R105 and R106, respectively. As shown in Fig. 6b, the values of  $I_{R58}$ ,  $I_{R105}$ , and  $I_{R106}$  increases with an increase in the stagnation plane temperature,  $T_w$ . Here, we consider the difference between the overall production and the overall reduction of  $N_2O$ , i.e.,  $I_{R58} - (I_{R105} + I_{R106})$ , and the value was shown in Fig. 6a. This value decreases monotonically with an increase in  $T_w$ . Also, this value reached almost constant value for  $T_w > 1500$  K. As shown in Fig. 5,  $N_2O$  increased when the stagnation plane temperature was lower than 1500 K. With a decrease in the stagnation plane temperature, the value of  $I_{R58}$  and  $I_{R105}$  almost linearly decreases. However, the values of  $I_{R106}$  decreases non-linearly with a decrease in  $T_w$ . The decrease in the  $N_2O$  reduction through R106 reduces at low temperature region, and large amount of  $N_2O$  remained in the product gas.

### 3.3 Effects of Equivalence Ratio on Product Gas Characteristics

Figure 2c represents a rapid increase in  $N_2O$  with a decrease in equivalence ratio. To clarify this characteristic, a similar analysis to section 3.2 was also conducted. Figure 7 represents the  $N_2O$  mole fraction at the stagnation plane for various equivalence ratio at the fixed stagnation plane temperature and mixture inlet velocity. The value of  $N_2O$  increases rapidly for  $\phi < 0.65$ .

Figure 8 represents variations of the integral value of the reaction rate,  $I_R$ , in terms of the equivalence ratio,  $\phi$ . As shown in Fig. 8a, the value of  $I_{R58} - (I_{R105} + I_{R106})$  increases with a decrease in the equivalence ratio, and this value also increases

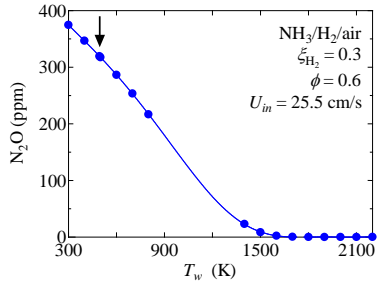


Figure 5: Effects of stagnation plane temperature on  $N_2O$  mole fraction. The condition indicated with the arrow corresponds to the stagnation plane temperature at the experimental condition. Here, no converged results were obtained between  $900 < T_w < 1300$  K.

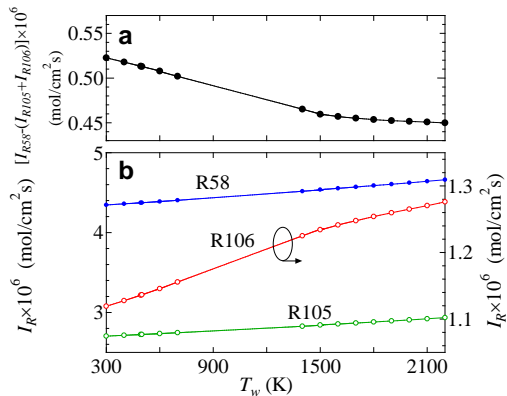


Figure 6: Integral value of the reaction rate of reaction  $R$ ,  $I_R$ , in terms of the stagnation plane temperature,  $T_w$ .

rapidly for  $\phi < 0.65$ . This trend was well related to the  $N_2O$  characteristics shown in Fig. 7. Figure 8b shows the variations of  $I_R$  for each reaction. The value of  $I_{R58}$  and  $I_{R105}$  reduces almost linearly with a decrease in equivalence ratio. However, the values of  $I_{R106}$  were small for leaner conditions. The decrease in  $I_{R106}$  induces the increase in  $N_2O$  as shown in Fig. 7. Therefore, the importance of R106 for  $N_2O$  emissions were suggested from numerical analysis with Gotama Mech.

## 4 Conclusions

Product gas characteristics of ammonia/hydrogen/air premixed laminar flames stabilized in stagnation flows were experimentally and numerically investigated. It was found that the mole fractions of NO of ammonia/hydrogen/air flames are greater than that of pure ammonia/air flames. Also, a trade-off relationship between NO and unburnt  $NH_3$  are observed at slightly rich condition, indicating that the rich-lean two-stage combustion may be applicable for this mixture. Also,  $N_2O$ , which has large global warming potential increases rapidly for very lean condition. To understand this characteristic, numerical simulation with a detailed reaction kinetic developed by Gotama et al. were conducted. The sensitivity analysis shows that these three reactions play an important role in  $N_2O$  production for the examined mixture: (R58)  $NH+NO = N_2O+H$ , (R105)  $N_2O+H = N_2+OH$ , and (R106)  $N_2O(+M) = N_2+O(+M)$ . In the case of low stagnation plane temperature and/or the small equivalence ratio cases, the overall reduction rate of  $N_2O$  through R106 decreases non-monotonically with a decrease in the stagnation plane temperature and the equivalence ratio. Therefore, a decrease in  $N_2O$  reduction to  $N_2$  through this

reaction causes large emission of  $N_2O$ .

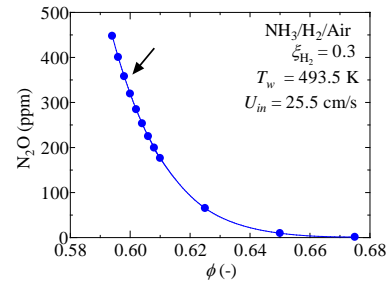


Figure 7: Effects of equivalence ratio on  $N_2O$  mole fraction. The condition indicated with the arrow corresponds to the equivalence ratio at the experimental condition.

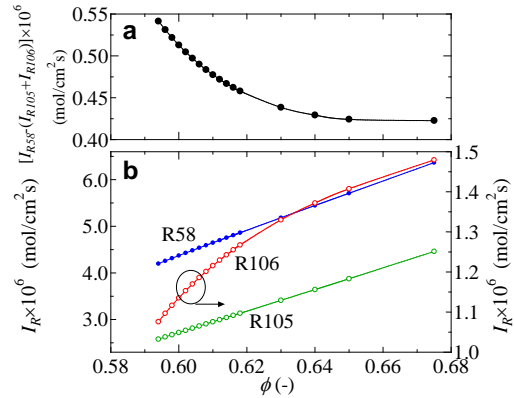


Figure 8: Integral value of the reaction rate of reaction  $R$ ,  $I_R$ , in terms of the equivalence ratio,  $\phi$

## 5 Acknowledgment

This work was partially supported by the Collaborative Research Project (J211026) of the Institute of Fluid Science, Tohoku University, and the Suzuki Foundation.

## References

- [1] [https://www.meti.go.jp/english/press/2021/0618\\_002.htm](https://www.meti.go.jp/english/press/2021/0618_002.htm)
- [2] H. Kobayashi, A. Hayakawa, K.D.K.A. Somarathne, E.C. Okafor, Proc. Combust. Inst., 37 (2019) 109-133.
- [3] A. Hayakawa, T. Goto, R. Mimoto, Y. Arakawa, T. Kudo, H. Kobayashi, Fuel, 159 (2015) 98-106.
- [4] A. Ichikawa, A. Hayakawa, Y. Kitagawa, K.D.K.A. Somarathne, T. Kudo, H. Kobayashi, Int. J. Hydrogen Energy, 40 (2015) 9570-9578.
- [5] A. Hayakawa, Y. Hirano, E.C. Okafor, H. Yamashita, T. Kudo, H. Kobayashi, Proc. Combust. Inst., 38 (2021) 2409-2417.
- [6] E.C. Okafor, M. Tsukamoto, A. Hayakawa, K.D.K.A. Somarathne, T. Kudo, H. Kobayashi, Proc. Combust. Inst., 38 (2021) 5139-5146.
- [7] <https://www.jccca.org/download/13266> (in Japanese).
- [8] A. Valera-Medina et al. Int J Hydro Energy 44(16) (2019), pp. 8615-8626.
- [9] A. Hayakawa, Y. Hirano, A. Ichikawa, K. Matsuo, T. Kudo, H. Kobayashi, Mech. Eng. J., 7 (2020) 19-00193.

[10] ANSYS CHEMKIN-PRO 19.0, 2017